Electromagnetic design and tuning of the four-vane radio frequency quadrupole with nonuniform intervane voltage profile

Takatoshi Morishita[*] and Yasuhiro Kondo
Japan Atomic Energy Agency (JAEA), Tokai, Naka, Ibaraki 319-1195, Japan

(Received 17 August 2020; accepted 6 November 2020; published 30 November 2020)

Equipartitioning is an efficient beam-dynamics design scheme also for radio frequency quadrupole (RFQ). To realize an equipartitioned RFQ, it is essential to reproduce the nonuniform intervane voltage profile required from the beam dynamics. We developed a cavity design and tuning method to this end. The dimensions of a voltage-ramped four-vane cavity were determined by a three-dimensional rf simulation. To produce the desired vane voltage profile, the longitudinal variation of the cross-sectional shape was adjusted using the least-squares method based on the simulated responses of the vane-base width to the quadrupole-mode field. In the low-level tuning, slug-tuner positions were determined based also on the least-squares solutions obtained from the simulated tuner responses to the field profile. Finally, the deviation of the quadrupole-mode field was within 1.5% from the design profile, and the mixed dipole modes were 1% of the quadrupole-mode field after only two iterations of tuner adjustment; they are sufficiently smaller than the requirement of 2%.

DOI: 10.1103/PhysRevAccelBeams.23.111003

I. INTRODUCTION

In recent high-intensity hadron accelerators, excessive beam loss is a potential cause of radio activation on the accelerator components. Therefore, the desired beam quality should be realized to suppress the unexpected beam loss to a sufficiently small fraction. To achieve this, the performance of the radio frequency quadrupole (RFQ) linac, which is the front-end accelerating structure of the high-intensity hadron linac, is essentially important. To satisfy the beam-quality requirements with an optimized length, we developed and demonstrated an RFQ for the Japan Proton Accelerator Research Complex (J-PARC) [1] H^- (negative hydrogen) linac based on the beam-oriented design scheme [2]. The equipartitioning beam-dynamics design is implemented to this RFQ, so this RFQ is called epRFQ.

In the beam-oriented design scheme, the intervane voltage V is no longer constant; it is ramped along the RFQ to satisfy the equipartitioning condition. To obtain the desired beam performance of the equipartitioned RFQ, it is very important to precisely reproduce the desired design voltage profile along the RFQ. This kind of nonuniform voltage profile is realized using higher-order mode mixing driven by local resonant frequency perturbations [3], and, in many cases, the frequency perturbations are usually introduced by using slug tuners [4,5]. The response function of the slug tuners to the field profile has been calculated based on analytical methods such as a waveguide model [3] and an equivalent-circuit model [5–7]. The analytical method is good for understanding the principle; however, the parameters, such as the resonant frequencies of each mode, should be carefully calculated to obtain a proper response function. Sometimes, it is difficult, or the model becomes too complicated, to derive the response function if detailed structures such as dipole stabilizing rods (DSRs) on the cavity ends [8,9] are implemented. Another way to derive the response function is to measure the actual response of the tuners one by one [10], but it is time consuming. Usually, tuning is conducted with exposure to the atmosphere, so the tuning time should be as short as possible.

On the other hand, the remarkable progress of the finite element method (FEM) analysis software enables us to utilize three-dimensional (3D) models for very high-precision radio frequency (rf) designs. Once a 3D model is created, it is very easy to derive the response function of the tuners, and it is also easy to implement the realistic structures of the cavity. Furthermore, it becomes possible to obtain a demanded V profile in the design phase in a comprehensive manner, without using slug tuners. We established a method to realize the ramped V profile required from the equipartitioning beam-dynamics design by making full use of the FEM tool. This also significantly simplifies the tuning procedure and shortens the tuning time. In this paper, we describe in detail the procedure for this rf design and tuning method developed for epRFQ.

[*]takatoshi.morishita@j-parc.jp

TABLE I. Main parameters of epRFQ.

Resonant frequency	324 MHz
Accelerated particle	H^-
Peak beam current	>50 mA
Input energy	0.05 MeV
Output energy	3 MeV
Output transverse normalized rms emittance	<0.25π mm mrad
Repetition rate	50 Hz
rf pulse length	600 μs
rf duty factor	3%
Number of cells	285
Vane length	3.1 m
V	61.3–143 kV
$E_{\max}$	30.3 MV/m (1.70 Kilpatrick)
r_0	2.6–6.2 mm
Transverse vane-tip curvature	$0.75r_0$
Longitudinal vane profile	Two-term potential
rf structure	Four-vane
Dipole suppressor	DSR

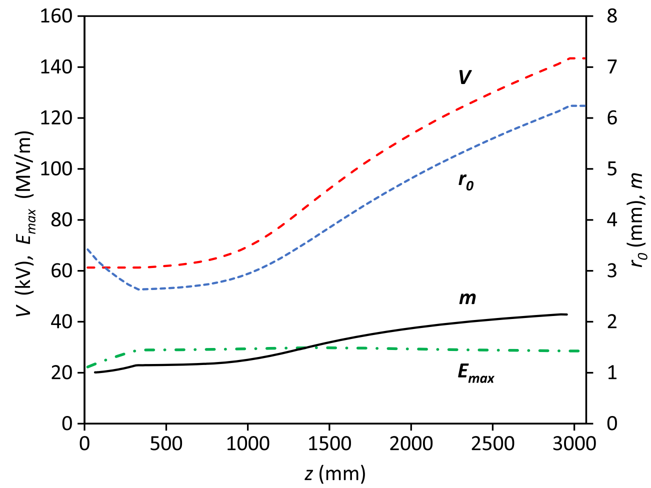

FIG. 1. Cell parameters of epRFQ as functions of the longitudinal position z for V, $E_{\max}$, r_0, and modulation factor m.

The beam-dynamics design and the beam performance of epRFQ are presented in a separate paper [2]. This design method is quite suitable to obtain the required V profile of the equipartitioned RFQ precisely, but, of course, it can be used generally for every four-vane RFQ, especially high-intensity RFQs, which tend to be long.

This paper is organized as follows. First of all, the procedures of the electromagnetic design of epRFQ are described in Sec. II. The cavity structure of epRFQ and apparatus for low-level tuning are presented in Sec. III. The low-level tuning procedures are shown in Sec. IV with the final results of the field profile and rf properties. Finally, a conclusion is given in Sec. V.

II. rf DESIGN OF THE RFQ CAVITY

Table I shows the main parameters of epRFQ, and Fig. 1 is a plot of the cell parameters as functions of the longitudinal position z along the RFQ. As described in the previous section, this RFQ adopts the equipartitioning design scheme. Therefore, the average bore radius r_0 is ramped along the RFQ to satisfy the equipartitioning condition with an almost constant maximum surface field $E_{\max}$. Consequently, the V is also increased.

The 3D dimensions of the voltage-ramped four-vane cavity were determined in the following three steps. First of all, the initial two-dimensional (2D) cross-sectional shapes for each different r_0 were determined by keeping the resonant frequency f_0 constant using RFQFISH [11] (step 1). However, with constant f_0, the V must also be a constant. To obtain the desired V profile, the higher-order modes should be mixed by introducing an appropriate frequency perturbation along z. This frequency perturbation was realized by changing the half width of the vane base W_b along the RFQ. The geometric structure of W_b is shown in Figs. 2 and 3 in the following subsections. For tuning of the V profile, we used a response matrix obtained from a simulated electromagnetic field using a 3D model without vane-tip modulation. The response function was inversely solved by the least-squares method to derive W_b which reproduce the desired V profile (step 2). Finally, the distortion of the V profile due to the vane-tip modulations was corrected by the fine-tuning of W_b (step 3). The details of each procedure are described in the following subsections.

A. Determination of the initial 2D cross-sectional shapes

RFQFISH was used to obtain the initial 2D cross-sectional shapes of a quadrant. The vane-tip parameters were sampled at 50 z positions, and the W_b's were tuned for r_0 of each sectional shape to keep f_0 to be 324 MHz. The cross-sectional shapes obtained at $z = 516$ and 3009 mm correspond to the maximum and minimum W_b's, respectively, and are shown in Fig. 2.

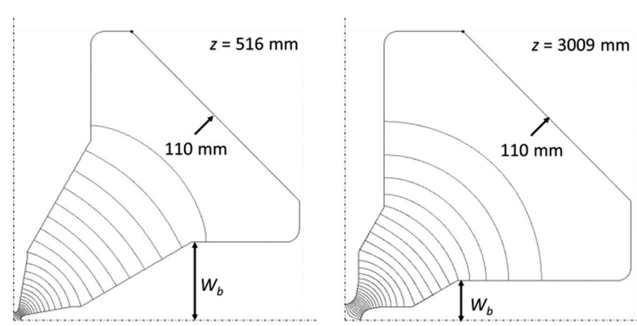

FIG. 2. Cross-sectional shapes of the cavity at $z = 516$ (left) and 3009 mm (right) obtained with RFQFISH. The distance from the cavity center to the wall is 110 mm.

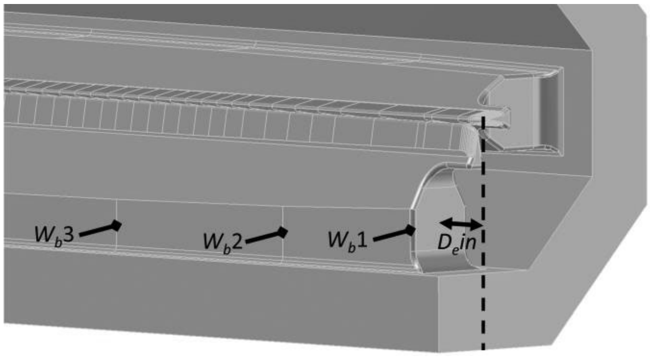

FIG. 3. Vane model for tuning the W_b's and the D_e's. Actual eigenmode calculation was done in one quadrant assuming fourfold symmetry.

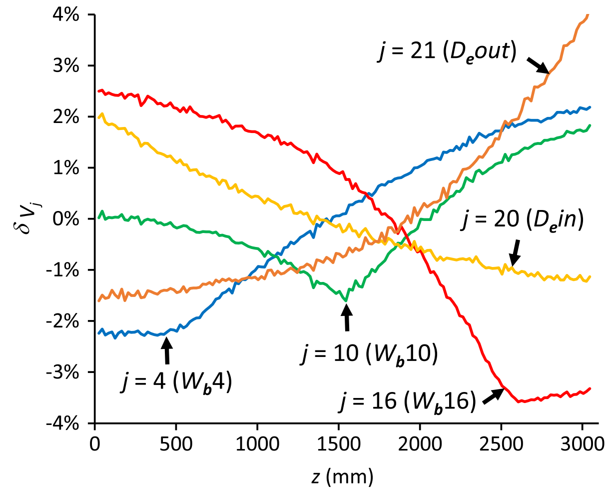

FIG. 4. Normalized deviations of the intervane voltage δV_j for parameters of W_b's and D_e's. For W_b's, only three curves from a total of 19 W_b's are plotted for graph visibility.

B. Tuning of 3D dimensions to produce the design intervane voltage profile

In the next step, W_b was tuned to obtain the desired V profile by using the 3D rf simulation. A 3D model of a quadrant was made in CST Microwave Studio (MWS) [12] based on the sectional shapes obtained in the previous subsection. In this model, the W_b's at 19 z positions with the same interval were parameterized, and the vane skirt was shaped by linearly interpolating the W_b's, as shown in Fig. 3. The initial values of the W_b's were set to be the results obtained with RFQFISH. At both ends of the cavity, the vane-end-undercut depths D_e's are also parameterized. The initial values for D_e's were obtained by scanning the D_e's of a model limited to the end part, so that the frequency of this model is 324 MHz. The electromagnetic field of the TE210 mode was calculated by the eigenmode solver of MWS to obtain the V profile with the initial dimensions. The V at a particular z position was evaluated by integrating the calculated electric field from the cavity center to the vane tip. The simulation accuracy was checked by confirming the resonant frequencies and the field profiles with different fineness of the tetrahedral mesh. The calculation time to obtain one eigenmode result was typically one hour with approximately 1.4 million mesh cells.

With this initial condition, the calculated V profile is almost flat because of the constant f_0 along the cavity. From the initial condition, the W_b's and D_e's were tuned to obtain the design V profile. To evaluate the response of the V profile to the variation of the W_b's and D_e's, these parameters were independently changed by 1 mm in the MWS calculation. The normalized vane voltages $\tilde{V}_{ij}$ for the model with a 1-mm variation of the jth parameter ($j = 1$–19 are for the W_b's and 20 and 21 are for the D_e's) were calculated at totally 152 points along the z direction with an interval of 20 mm ($i = 1$–152). Each $\tilde{V}_j$ was normalized by the averaged value over the 152 points. Then, the responses δV_{ij} to the jth variation were obtained as $\tilde{V}_{ij} - \tilde{V}_{i,\mathrm{org}}$. The values of δV_{ij} were from 3% to 9% for the W_b's and those for the D_e were from 3% to 6%. The response functions of the sampled variations are shown in Fig. 4. The fluctuation of each curve comes from the finite mesh size, and it is typically 0.1%. No smoothing was applied, and the obtained δV_{ij} was directly used for the tuning process.

Suppose that X is an $i \times j$ matrix with elements of δV_{ij} and A is a 21-dimensional variation vector of the W_b's and D_e's, and then a 152-dimensional deviation vector Y of the V profile can be written as

$$Y = XA. \tag{1}$$

If Y is the difference between the normalized design voltage profile $\tilde{V}_{i,\mathrm{design}}$ and the initial one, the variation vector A from the initial value can be obtained as a least-squares solution by

$$A = X^{+}Y, \tag{2}$$

$$X^{+} = (X^T X)^{-1} X^T, \tag{3}$$

where X^{+} is a pseudoinverse matrix. The V profile converged to within $\pm 0.2\%$ of the design V profile after two iterations. During these iterations, all parameters were uniformly shifted to adjust the frequency. Figure 5 shows the V profiles and the W_b's before and after tuning. The variations of $D_e$in and $D_e$out was 44.80 and 41.65 mm, respectively.

C. Correction of the distortion due to the modulations

The final process is the modulation correction. To this end, it is necessary to perform the electromagnetic field

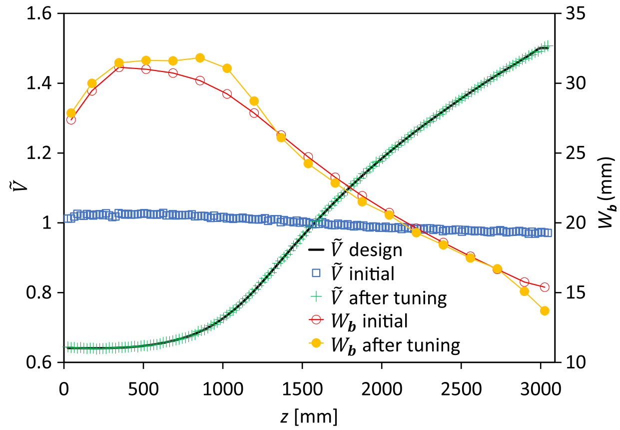

FIG. 5. Normalized V profiles and W_b's before and after tuning.

simulation with a 3D model implementing the vane-tip modulations, and much finer mesh is required to evaluate the electric field near the modulated vane tip. Therefore, the procedure described in Sec. II B is not able to be conducted within a realistic time. Instead, a magnetic field H profile at 78 mm from the cavity center, where the magnetic field is dominant, was used as the target profile of the modulation correction, as usually used in the low-level tuning phase. The principle of the correction itself is the same as that described in Sec. II B. The calculated H profile of the model without modulations after the tuning in the previous subsection was regarded as the target magnetic field profile. The response of the H profile to each parameter was constructed in the same way as the response matrix of the V profile. The calculated normalized magnetic field profile $\tilde{H}$ and the variations of W_b's and D_e's are shown in Fig. 6. Note that we adopted the two-term longitudinal vane profile for epRFQ [2]; therefore, the distortion due to the modulation is relatively small. The CST calculation indicated that the implementation of the modulation

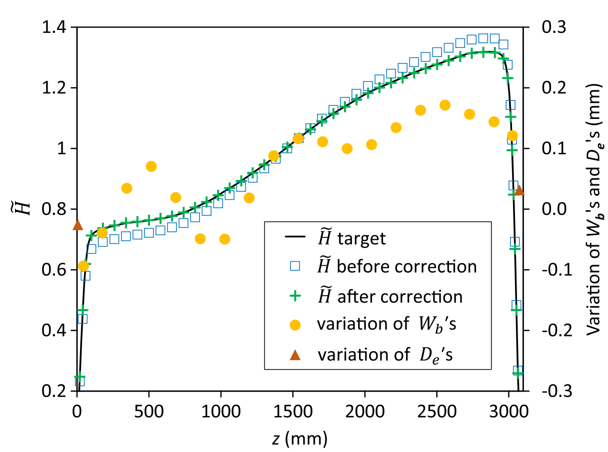

FIG. 6. Magnetic field profiles before and after the vane-tip modulation correction. The closed markers show the variations required for the correction.

induces approximately 5% field tilt. The required variations of the W_b's and D_e's were fine-tuning level, namely, less than 0.2 mm.

After finishing all the procedures in this section, the 3D model became completed. It was passed to the manufacturer, and then a computer-aided design (CAD) model for fabrication was made based on this 3D model. In this fabrication model, the vane skirts are smoothed by a spline curve. After developing the detailed mechanical design (i.e., actual vane-skirt shape and vane splitting) into three modules, the CAD model was imported into CST MWS again, and the electromagnetic field was confirmed. The field differences from the original rf design model were within the mesh errors.

III. CAVITY STRUCTURE AND LOW-LEVEL TUNING APPARATUS

The fabrication technique of the epRFQ is based on that we established through the development of the former J-PARC RFQ [13]. The epRFQ cavity consists of three longitudinally divided modules. The vane lengths of the modules are 1024.7, 1029.5, and 1018.9 mm, respectively. Each module consists of upper and lower major vanes and left and right minor vanes as shown in Fig. 7.

The upper right quadrant is denoted as Q1, the upper left is denoted as Q2, the lower left is denoted as Q3, and the lower right is denoted as Q4. The right and left are defined as views from the upstream. The machining accuracy of the vane-tip structure was measured to be less than 0.02 mm with a coordinate measuring machine. The major and minor vanes were joined by vacuum brazing using Ag72–Cu28 eutectic alloy.

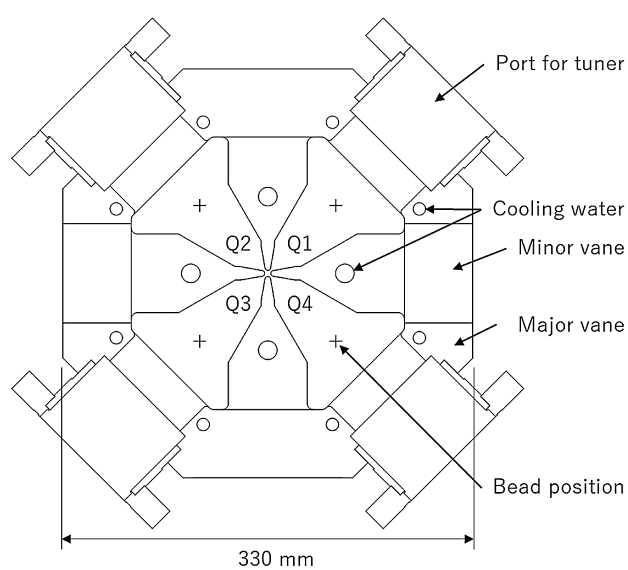

FIG. 7. Cross-sectional view (from upstream) of the epRFQ cavity.

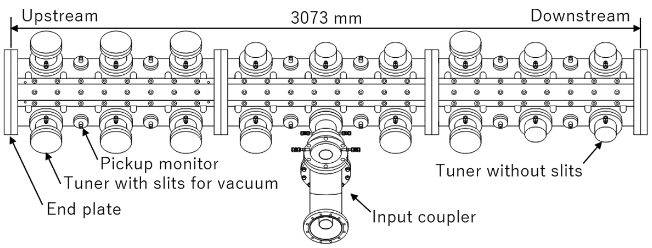

FIG. 8. Side view of the cavity with high-power tuners and a high-power coupler.

Figure 8 shows a side view of epRFQ. The cavity is equipped with 36 ports for 35 slug tuners and one loop-type input coupler. The diameter of the tips of the slug tuners and the coaxial waveguide of the input coupler inserted into the cavity is 78 mm. Nine ports are distributed longitudinally with equal intervals in each quadrant. The slug tuners at the upstream three ports and the seventh port of each quadrant and fourth and sixth ports of Q4 are combined with vacuum ports [14]; thus, the tips of the tuners are slit, as shown in Fig. 9. The tips of the other 17 tuners are plane plugs. The input coupler is located at the center port of Q4. Each end plate has four DSRs with a 14 mm diameter to adjust the distances of the nearby dipole modes from the operating mode. 24 pickup monitors were installed to measure the field profile during the operation.

In the low-level tuning, adjustable low-level tuners, DSRs, and a coupler were attached to the cavity. The tuner and coupler used for the low-level tuning are shown in Fig. 10. The insertion depths of the slugs and the coaxial waveguide can be adjusted manually, and they are measured with digital linear scales. The tips of the tuners at the vacuum ports are slit the same as the high-power tuners to reproduce the field leakage to the slits. The loop of the coupler is exchangeable for the coarse adjustment of the coupling constant. Five different loop sizes were prepared. Fine-tuning of the coupling constant was done by rotating the coaxial waveguide itself. A reducer from the 77D coaxial waveguide to the type-N connector was attached to the coupler. The slug and the coaxial waveguide are electrically contacted with the support cylinders via finger contactors, and the support cylinders are directly contacted with the spot facing of the ports.

The configuration of the endplates for the low-level tuning is shown in Fig. 11. Temporary assembled copper plates and stainless-steel flanges, which are actual parts of

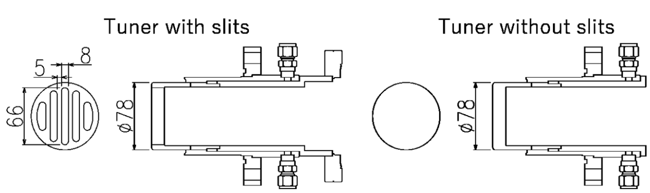

FIG. 9. Slug tuners with and without slits for vacuum pumping.

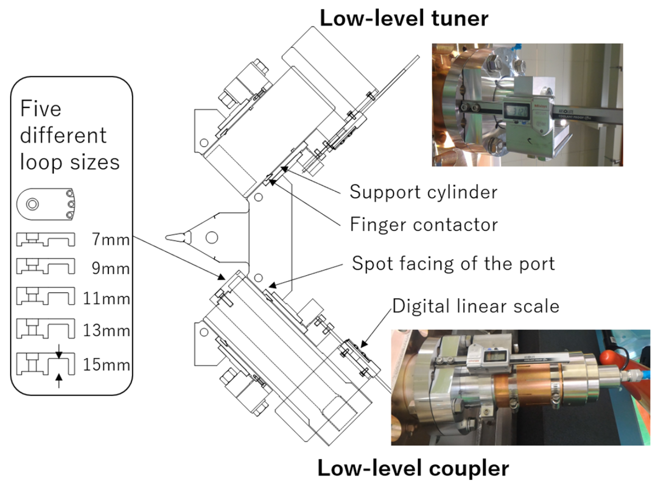

FIG. 10. Tuner and coupler used for low-level tuning.

the high-power end plates, were used for the low-level tuning. Dummy aluminum DSRs supported by guide blocks are inserted through the copper plates. Four through holes to penetrate the beads are drilled on each copper plate. The copper plates, the flanges, and the finalized copper DSRs were brazed together as completed high-power end plates after determining the rod lengths. The holes for the bead measurement were plugged with stainless-steel flanges and Viton O rings. After the low-level tuning, the low-level tuners and coupler were replaced by fixed tuners and couplers that have cooling structures, electrical contacts, and vacuum seal structures for high-power operation.

For the field tuning, H profiles of all quadrants were measured using the bead-perturbation method. Figure 12 shows the setup of this measurement. Aluminum cylinders with a diameter of 10 mm and a length of 10 mm were used for each quadrant. The bead positions are equidistant from the vane and are at 78 mm from the cavity center, which is the same position as mentioned in Sec. II C. Driver units for the beads were attached at each end of the platform.

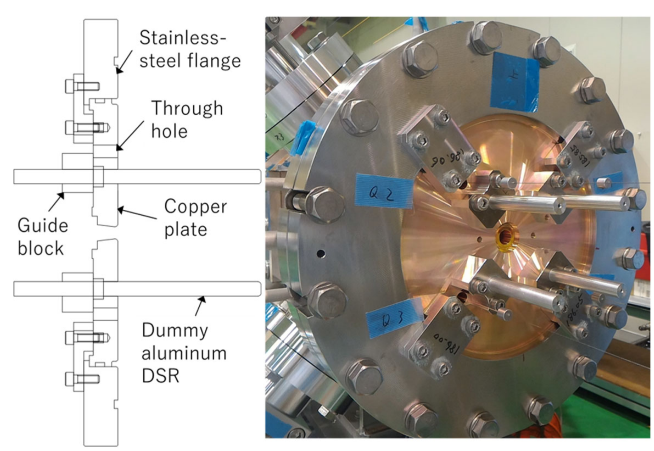

FIG. 11. Configuration of the end plate for the low-level tuning.

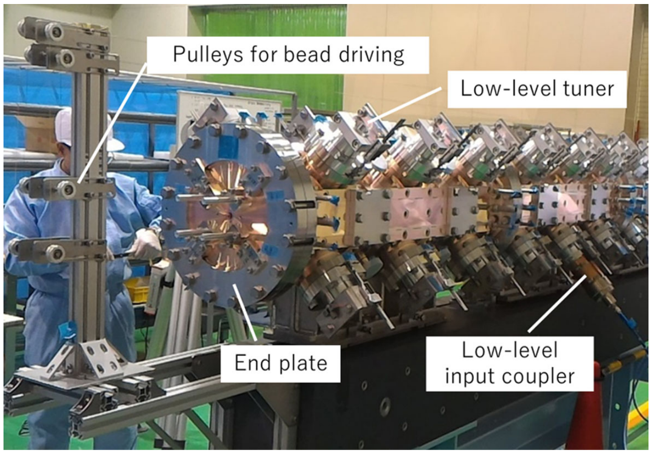

FIG. 12. Setup of the bead-perturbation measurement.

With scanning the beads individually for all quadrants, the phase shifts, which are proportional to the square of the H strength at the bead, were measured by a vector network analyzer. The rf power was fed to the coupler and returned from the pickup monitor. The phase shifts were measured typically once every 0.2 s, and the typical measurement time for one quadrant was 2 min.

IV. LOW-LEVEL TUNING

A. Tuning procedure

In the low-level tuning, frequency and field-profile tuning of operating mode (TE210), separation adjustment of the dipole modes (TE111 and TE112) from the operating mode, and coupling adjustment of the input coupler were performed. Since all the assumed corrections to the field profile are already included in the design, what to do in the low-level field tuning is only the correction of machining and assembling errors. The deviation of the quadrupole field profile from the design and the dipole-mode mixing to the quadrupole mode were targeted to be within 2%. The tuning procedure was as follows.

First of all, all tuner ports were equipped with the low-level tuners, and the low-level tuners and DSRs were set to the default positions. The default positions for tuners were decided to cancel out the frequency difference induced by the detail structure of the tuners, such as the clearance between the slug and the cavity and the vacuum slits, implemented in the MWS model. The default insertion of the slit and nonslit tuners from the cavity wall were 1.9 and 0.9 mm, respectively. Then the low-level tuner at the coupler port was replaced by the low-level coupler. The insertion depth of the coupler was manually adjusted to maintain the resonant frequency. The default length of the DSR was 130 mm, which was determined with the MWS calculation so that the TE210 mode is centered between the TE111 and TE112 modes.

With the default settings, the measured frequency of the operating mode was 0.130 MHz lower than the target frequency. The target frequency was 323.945 MHz with the condition that the cavity temperature was 20 °C and the cavity was filled with 15% humidity air. This frequency corresponds to 324.000 MHz with 27 °C and the vacuum inside the cavity. The correction factor of the cavity temperature and humidity inside the cavity are −0.039 and +0.094 MHz, respectively. The measured H profile with this condition is shown in Fig. 13. The deviations of the quadrupole field were 3% from the design profile, and the mixed dipole modes were 8% of the quadrupole field.

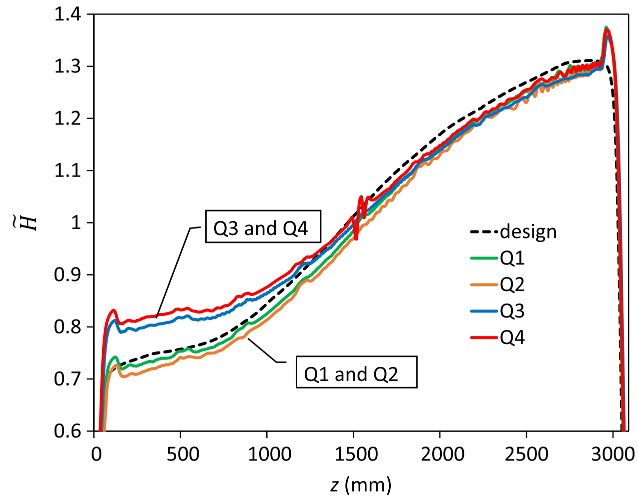

FIG. 13. Measured H profile for all the quadrants before tuning. The dashed line is the design profile obtained in Sec. II.

After the rough adjustment of the tuners, the quadrupole mode tilt and dipole-mode mixing of approximately 2% were easily obtained. This signifies the advantage of our rf design scheme, as emphasized above. The insertion depths of tuners were −1.5 to +1.8 mm. The length of the DSR was adjusted to be 125 mm so that the operating mode was around the center of the nearby dipole modes. The nearest dipole-mode frequency was 4.1 MHz, which is lower than that of the TE210 mode, whereas the simulated separation conducted with a DSR length of 130 mm was 4.5 MHz.

The small backlashes between the low-power DSRs and the guide blocks may induce large position errors of the DSR tips due to a leverage effect; this seriously affects the field profile. To prevent this, the end plates were finalized to be high-power end plates before the following final tuning.

After replacing to the high-power end plates, the coupling factor was adjusted by choosing the appropriate loop size and rotating the loop angle. The coupling factor was determined by measuring the reflection coefficient Γ as $\beta = (1+\Gamma)/(1-\Gamma)$. With a loop angle of 32° from the upright position, the target value of 1.7 was obtained. The nominal power dissipation of epRFQ is 380 kW, and beam loading at 60 mA is 180 kW. Hence, with this condition, $\beta = (380+180)/380 = 1.5$. The target value of 1.7 has a margin included in it. By rotating the loop angle of the high-power coupler, the coupling constant can be adjusted from 0 to 2.

Although the field profile had almost met the requirement, the fine-tuning of the slug tuners was conducted to obtain enough margins. This detail is described in the next subsection.

After all the tuning was finished, high-power tuners and coupler were fabricated and replaced the low-level ones. Then, the rf properties such as the field profile, frequency, and Q value of the operating mode and coupling factor were finally checked.

B. Fine-tuning of the field profile

The principle of fine-tuning is the same as the tuning of the cavity dimension parameters described in Sec. II. The responses of every quadrant to each tuner of a particular quadrant were evaluated using MWS. The response to the coupler insertion was assumed to be the same as that of the tuners. To evaluate the response function correctly, it is necessary to use a 3D model that has the DSRs included. The deviations of the H were evaluated by inserting the tuners of the MWS model with 1 mm individually. The normalized H profile of every quadrant with a 1-mm variation of the jth tuner ($j = 1$–9) in Q1 were calculated at sampled ith points along the z direction, and these are denoted as $\tilde{H}_{ij}^{Q1}$, $\tilde{H}_{ij}^{Q2}$, $\tilde{H}_{ij}^{Q3}$, and $\tilde{H}_{ij}^{Q4}$. Only the tuners of Q1 were surveyed assuming cyclic symmetry. Three sampling positions between each tuner were taken. Thus, the total number of the sampling points is 24 (i.e., $i = 1$–24). Each $\tilde{H}_{ij}$ was normalized by the averaged value over the $24 \times 4 = 96$ sampled points. The responses of $\delta\tilde{H}_{ij}$ to the jth tuner variation was obtained as $\tilde{H}_{ij} - \tilde{H}_{i,\mathrm{org}}$. By comprising the tuner variation vectors A_{Hj} and the magnetic field deviation vectors Y_{Hi} of each quadrant, the relationship between the A_H and Y_H can be represented by using one response matrix X_H as

$$\begin{pmatrix} Y_{Hi}^{Q1} \\ Y_{Hi}^{Q2} \\ Y_{Hi}^{Q3} \\ Y_{Hi}^{Q4} \end{pmatrix} = \begin{pmatrix} \delta\tilde{H}_{ij}^{Q1} & \delta\tilde{H}_{ij}^{Q4} & \delta\tilde{H}_{ij}^{Q3} & \delta\tilde{H}_{ij}^{Q2} \\ \delta\tilde{H}_{ij}^{Q2} & \delta\tilde{H}_{ij}^{Q1} & \delta\tilde{H}_{ij}^{Q4} & \delta\tilde{H}_{ij}^{Q3} \\ \delta\tilde{H}_{ij}^{Q3} & \delta\tilde{H}_{ij}^{Q2} & \delta\tilde{H}_{ij}^{Q1} & \delta\tilde{H}_{ij}^{Q4} \\ \delta\tilde{H}_{ij}^{Q4} & \delta\tilde{H}_{ij}^{Q3} & \delta\tilde{H}_{ij}^{Q2} & \delta\tilde{H}_{ij}^{Q1} \end{pmatrix} \begin{pmatrix} A_{Hj}^{Q1} \\ A_{Hj}^{Q2} \\ A_{Hj}^{Q3} \\ A_{Hj}^{Q4} \end{pmatrix}, \tag{4}$$

by assuming cyclic symmetry. If Y_H is the residual of the measured H profile to the design profile, the insertion depths of the tuners can be determined as a least-squares solution by solving Eq. (4) inversely, $A_H = X_H^{+} Y_H$, like Eqs. (2) and (3). The frequency shift due to the profile tuning was corrected by applying a uniform offset to all the tuners in each iteration.

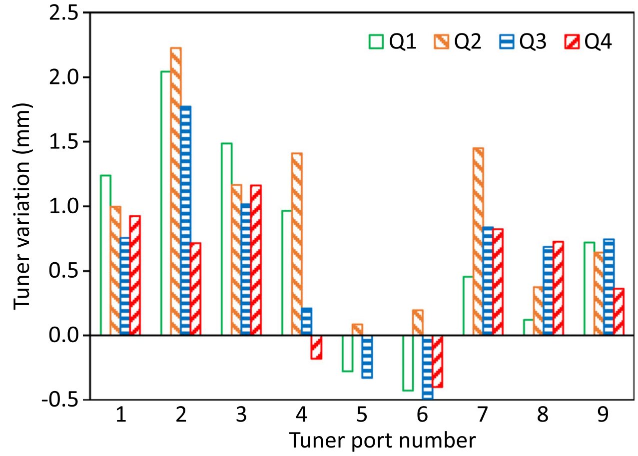

FIG. 14. Tuner insertion depths after low-level tuning. Port number 5 in Q4 is for the input coupler.

After only two iterations, the field profiles with deviations of ±1.5% from the designed profile of each quadrant were obtained. The final tuner variations from the default position were from −0.5 to 2.4 mm, as shown in Fig. 14. Figure 15 shows the measured field profile and the evaluated deviation of the quadrupole mode from the design and dipole-mode

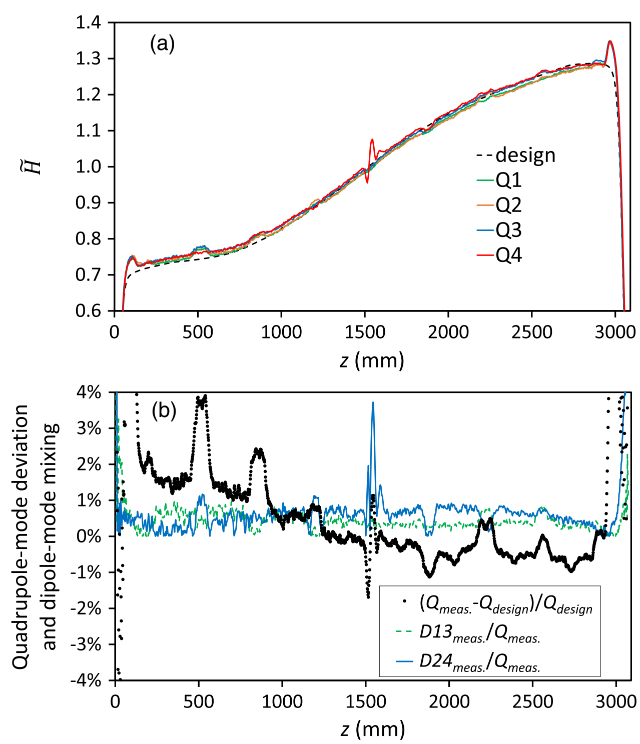

FIG. 15. (a) The measured H profile for all quadrants. The dashed line is the target profile as obtained in Sec. II. (b) The quadrupole-mode deviation and the dipole-mode mixing were derived from the measured magnetic fields.

TABLE II. Final rf characteristics of epRFQ.

Parameter	Value	Note
Frequency at 27 °C, vacuum	324.001 MHz	The design frequency is 324.000 MHz.
Nearest dipole-mode frequency	319.9 MHz	Operating mode locates between the TE111 and TE112 modes.
Coupling factor	1.70	The rotating angle of the coupling loop is 32°.
Unloaded Q value	9500	3D simulated value is 10400, using a model without the modulation.
Expected peak power	380 kW	Based on the measured Q value and the calculated vane voltage by the simulation.

mixing after replacing to the high-power tuners and coupler. The measured quadrupole field along z was derived as $Q_{\mathrm{meas}}(z) = [\tilde{H}(z)^{Q1}_{\mathrm{meas}} + \tilde{H}(z)^{Q2}_{\mathrm{meas}} + \tilde{H}(z)^{Q3}_{\mathrm{meas}} + \tilde{H}(z)^{Q4}_{\mathrm{meas}}]/4$. The dipole-mode elements were derived as $D13_{\mathrm{meas}}(z) = |\tilde{H}(z)^{Q1}_{\mathrm{meas}} - \tilde{H}(z)^{Q3}_{\mathrm{meas}}|/2$ and $D24_{\mathrm{meas}}(z) = |\tilde{H}(z)^{Q2}_{\mathrm{meas}} - \tilde{H}(z)^{Q4}_{\mathrm{meas}}|/2$. Local bumps observed are due to the disturbance by the tuners, DSRs, and coupler. Finally, the deviation of the quadrupole-mode field was within 1.5% from the design profile, and the mixed dipole modes were 1% of the quadrupole-mode field. Table II summarizes the final rf characteristics with the high-power parts. Enough characteristics for epRFQ were achieved.

V. CONCLUSION

The rf design and tuning method for the RFQ implementing the equipartitioning beam dynamics was developed. To realize the equipartitioned RFQ, it is essentially important to reproduce the required intervane voltage profile. To this end, the 3D cavity shape was determined with the full use of the electromagnetic simulation. In both rf design and low-level tuning, the rf field response to the tuning knobs was calculated using rf simulation, and the required settings of the knobs were derived as least-squares solutions using the pseudoinverse matrix. In the low-level tuning, the field profile was tuned with longitudinally distributed slug tuners. The careful rf design enabled very quick tuning process. As a result, the error of the quadrupole-mode field was within 1.5% from the design profile, and the mixed dipole modes were 1% of the quadrupole-mode field, which satisfied the requirement of 2%. The validity of this design and tuning procedure was proven by the excellent beam performance of epRFQ [2]. This procedure can be used universally for all the four-vane RFQs, especially long RFQs whose length is several times more than the wavelength.

ACKNOWLEDGMENTS

The authors express their thanks to Mr. Kyusaku Higa and Mr. Tomei Sugano of Mitsubishi Heavy Industries Machinery Systems, Ltd., for the fabrication of the cavity with attentive quality control. The authors are also grateful to Dr. Hidetomo Oguri and Dr. Michikazu Kinsho of JAEA, Dr. Kazuo Hasegawa of QST, and Professor F. Naito of KEK for their continuous support and encouragement.

[1] K. Hasegawa, N. Hayashi, H. Oguri, K. Yamamoto, M. Kinsho, Y. Yamazaki, F. Naito, T. Koseki, N. Yamamoto, and M. Yoshii, Performance and status of the J-PARC accelerators, in *Proceedings of IPAC2018, Vancouver, BC, Canada* (2018), pp. 1038–1040.

[2] Y. Kondo, T. Morishita, and R. A. Jameson, Development of a radio frequency quadrupole linac implemented with the equipartitioning beam dynamics scheme, Phys. Rev. Accel. Beams **22**, 120101 (2019).

[3] L. M. Young, Tuning and stabilization of RFQ's, in *Proceedings of the Linear Accelerator Conference 1990, Albuquerque, New Mexico, USA* (1990), pp. 530–534.

[4] L. M. Young and L. Rybarcyk, Tuning the LEDA RFQ 6.7 MeV accelerator, in *Proceedings of the 19th International Linear Accelerators Conference, Chicago, IL, 1998* (NTIS, Springfield, VA, 1998), pp. 270–272.

[5] A. Palmieri, F. Grespan, P. Mereu, D. Dattola, and G. Cotto, The IFMIF RFQ real-scale aluminum model: RF measurements and tuning, in *Proceedings of the International Particle Accelerator Conference, Kyoto, Japan* (ICR, Kyoto, 2010), pp. 603–605.

[6] A. France and F. Simons, Theoretical analysis of a real-life RFQ using a 4-wire line model and the theory of differential operators, in *Proceedings of the 8th European Particle Accelerator Conference, Paris, 2002* (EPS-IGA and CERN, Geneva, 2002), pp. 957–959.

[7] A. Palmieri, F. Grespan, and A. Pisent, Perturbation analysis on a four-vane RFQ, in *Proceedings of the International Particle Accelerator Conference, Kyoto, Japan* (ICR, Kyoto, 2010), pp. 606–608.

[8] L. M. Young, An 8-meter-long coupled cavity RFQ linac, in *Proceedings of the 17th International Linear Accelerator Conference (LINAC-1994), Tsukuba, Japan, 1994* (KEK, Tsukuba, Japan, 1994).

[9] F. Grespan, A. Pisent, and A. Palmieri, Dipole stabilizers for a four-vane high current RFQ: Theoretical analysis and experimental results on a real-scale model, Nucl. Instrum. Methods Phys. Res., Sect. A **582**, 303 (2007).

[10] B. Koubek, A. Grudiev, and M. Timmins, rf measurements and tuning of the 750 MHz radio frequency quadrupole, Phys. Rev. Accel. Beams **20**, 080102 (2017).

[11] J. H. Bilen and L. M. Young, Poisson Superfish, Los Alamos National Laboratory Report No. LA-UR-96-1834, 1996.

[12] CST Studio Suite, Computer Simulation Technology (CST), https://www.3ds.com/products-services/simulia/.

[13] Y. Kondo, T. Morishita, K. Hasegawa, E. Chishiro, K. Hirano, T. Hori, H. Oguri, F. Sato, T. Sugimura, H. Kawamata, F. Naito, Y. Fukui, K. Futatsukawa, and K. Nanmo, High-power test and thermal characteristics of a new radio-frequency quadrupole cavity for the Japan Proton Accelerator Research Complex linac, Phys. Rev. Accel. Beams **16**, 040102 (2013).

[14] T. Morishita, Y. Kondo, H. Oguri, and K. Hasegawa, Vacuum properties and operation stability of the radio-frequency quadrupole accelerator in Japan Proton Accelerator Research Complex linac, J. Vac. Sci. Technol. A **35**, 041602 (2017).